Role of commensurate and incommensurate low-energy excitations in the paramagnetic to hidden-order transition of URu$_2$Si$_2$

P. G. Niklowitz,[1,*] S. R. Dunsiger,[2] C. Pfleiderer,[3] P. Link,[4] A. Schneidewind,[5] E. Faulhaber,[4] M. Vojta,[6] Y.-K. Huang,[7] and J. A. Mydosh[8]

[1]*Department of Physics, Royal Holloway, University of London, Egham TW20 0EX, United Kingdom*
[2]*Center for Emergent Materials, Ohio State University, Columbus, Ohio 43210, USA*
[3]*Physik Department, Technische Universität München, 85748 Garching, Germany*
[4]*Heinz Maier-Leibnitz Zentrum, Technische Universität München, Lichtenbergstrasse 1, 85748 Garching, Germany*
[5]*Jülich Centre for Neutron Science at Heinz Maier-Leibnitz Zentrum, Forschungszentrum Jülich GmbH, Lichtenbergstrasse 1, 85748 Garching, Germany*
[6]*Institut für Theoretische Physik, Technische Universität Dresden, 01062 Dresden, Germany*
[7]*Van der Waals-Zeeman Institute, University of Amsterdam, 1018XE Amsterdam, Netherlands*
[8]*Kamerlingh Onnes Laboratory, Leiden University, 2300RA Leiden, Netherlands*

We report low-energy inelastic neutron scattering data of the paramagnetic (PM) to hidden-order (HO) phase transition at $T_0 = 17.5$ K in URu$_2$Si$_2$. While confirming previous results for the HO and PM phases, our data reveal a pronounced wave-vector dependence of low-energy excitations *across* the phase transition. To analyze the energy scans we employ a damped harmonic oscillator model containing a fit parameter $1/\Gamma$ which is expected to diverge at a second-order phase transition. Counter to expectations the excitations at $\vec{Q}_1 \approx (1.4,0,0)$ show an abrupt steplike suppression of $1/\Gamma$ below T_0, whereas excitations at $\vec{Q}_0 = (1,0,0)$, associated with large-moment antiferromagnetism (LMAF) under pressure, show an enhancement and a pronounced peak of $1/\Gamma$ *at* T_0. Therefore, at the critical HO temperature T_0, LMAF fluctuations become nearly critical as well. This is the behavior expected of a "supervector" order parameter with nearly degenerate components for the HO and LMAF leading to nearly isotropic fluctuations in the combined order-parameter space.

I. INTRODUCTION

For nearly 30 years one of the most prominent unexplained properties of f-electron materials has been the phase transition in URu$_2$Si$_2$ at $T_0 \approx 17.5$ K into a state referred to as "hidden order" (HO) [1–4] as the nature of the order parameter remains unknown. The discovery of the HO was soon followed by the observation of a small antiferromagnetic moment (SMAF), $m_s \approx 0.01$–$0.04\mu_B$ per U atom [5], then believed to be an intrinsic property of the HO. The observation of a large-moment antiferromagnetic phase (LMAF) with $m_s \approx 0.4\mu_B$ [6] *under pressure* consequently prompted intense theoretical efforts to connect the LMAF with the SMAF and the HO. However, muon spin resonance, NMR, Larmor, and magnetic neutron diffraction experiments suggested that the apparent SMAF is a result of the presence of LMAF in a small sample volume fraction [7–10]. Studies of the pressure-temperature phase diagram of URu$_2$Si$_2$ consistently establish the existence of a bicritical point, which implies that HO and LMAF break *different* symmetries [9,11–14]. To explain these properties, exotic scenarios of the HO have been proposed, such as incommensurate orbital currents [15], helicity order [16], multipolar order [17–20], order due to dynamic symmetry breaking [21], the so-called hastatic order [22], and spin-orbit density waves [23,24]. Indications of breaking of the fourfold tetragonal in-plane symmetry at T_0 have motivated the consideration of a spin-nematic state [25–28].

Inelastic neutron scattering has been essential for gaining microscopic insight into the nature of the HO (see, e.g., [29,30]). The existence of commensurate and incommensurate excitations in the HO at $\vec{Q}_0 = (1,0,0)$ and $\vec{Q}_1 \approx (1.4,0,0)$, respectively, has been known for quite a while [5]. The incommensurate excitations at $\vec{Q}_1$ are reported to exist in the HO and LMAF phases, with gaps of approximately 4 and 8 meV, respectively [31,32], and with a reduced gap [29,33] or even gapless nature [34] in the PM phase. The closing of the gap has been quantitatively linked to the specific-heat jump at T_0 [34]. In contrast, the commensurate excitations at $\vec{Q}_0$ have previously been observed only in the HO phase (gap of approximately 2 meV), and no critical behavior at T_0 has been reported [30,32]. Therefore, the link between excitations at $\vec{Q}_0$ and $\vec{Q}_1$ and the HO has remained unclear.

In this paper we present compelling evidence that the *commensurate* fluctuations at $\vec{Q}_0$ do not disappear right at T_0 but evolve in a way across the PM-HO transition, which allows us to interpret them as precursors of LMAF order. Further, the LMAF and HO fluctuations are clearly interrelated, and $\vec{Q}_{AF} = (0,0,1)$ is the most likely HO wave vector, while the incommensurate fluctuations at $\vec{Q}_1$ are mere bystanders. This is the result of a direct and quantitative comparison of the excitations at $\vec{Q}_0$ and $\vec{Q}_1$, which have been studied in a single neutron scattering experiment. Detailed temperature scans across the HO-PM phase transition at low energies turn out to be an ideal way to visualize in the raw data the existence of a clear qualitative difference in the behavior at $\vec{Q}_0$ and $\vec{Q}_1$. At the incommensurate $\vec{Q}_1$ position the gap is filled abruptly at T_0 upon heating, i.e., the low-energy excitations are enhanced in a

*philipp.niklowitz@rhul.ac.uk

steplike fashion upon entering the PM phase. In contrast, scans at the commensurate $\vec{Q}_0$ position show that the low-energy excitations are enhanced across a considerable temperature range and peak at T_0.

A detailed analysis of energy scans confirms that the fluctuations at $\vec{Q}_0$, which can be understood as precursors of LMAF order, become *almost critical* at the PM-HO transition, in addition to the expected critical fluctuations of the hitherto unidentified HO parameter. This is not expected in a standard scenario of competing order parameters for HO and LMAF, which break different symmetries. However, it is consistent with nearly isotropic fluctuations of a supervector order parameter as described in the discussion, which consists of components for both HO and LMAF. Isotropy in this order-parameter space would imply an emergent symmetry between both orders, which may be tested experimentally.

II. EXPERIMENT

The $2g$ single crystal studied was grown by means of an optical floating-zone technique at the Amsterdam/Leiden Center. High sample quality was confirmed via x-ray diffraction and detailed electron probe microanalysis. The mosaic spread is less than $1°$. Samples prepared from this ingot showed good resistance ratios (20 for the c axis and ≈ 10 for the a axis) and a high superconducting $T_c \approx 1.5\,K$. The magnetization of the large single crystal agreed very well with data shown in Ref. [35] and confirmed the absence of ferromagnetic inclusions. Most importantly, in our neutron scattering measurements we found an antiferromagnetic moment $m_s \approx 0.012\mu_B$ per U atom [9], which matches the smallest moment reported so far [36].

Inelastic neutron scattering measurements were carried out at the cold triple-axis spectrometer PANDA at Forschungs-Neutronenquelle Heinz Maier-Leitnitz (FRMII). The sample was mounted on a Cd-shielded Cu holder and oriented with $(h0l)$ as the horizontal scattering plane. PANDA was used in the W configuration with a vertically and horizontally focusing monochromator and analyzer and no collimation. The final wave vector was kept fixed at $1.55\,Å^{-1}$. Higher-order harmonics were removed from the scattered beam by a liquid-nitrogen-cooled Be filter, and monitor correction for higher-order neutrons was included. The temperature evolution of the low-energy excitations of URu$_2$Si$_2$ at commensurate $\vec{Q}_0$ and incommensurate $\vec{Q}_1$ was studied by low-energy scans at different temperatures. Most importantly, detailed temperature scans at $E = 0.5$ meV were carried out at each position.

A. Energy scans

Figure 1 shows typical energy scans for $\vec{Q}_0$ and $\vec{Q}_1$. At both positions scattering by considerably damped excitations is found for temperatures above T_0. At T_0 gaps begin to open up, and as T decreases further, the intensities of the excitations increase while the gaps widen. The spectrum is clearly gapped at low temperatures. At 3 K, low-energy excitations are detected at 2 meV at $\vec{Q}_0$ and just above 4 meV at $\vec{Q}_1$.
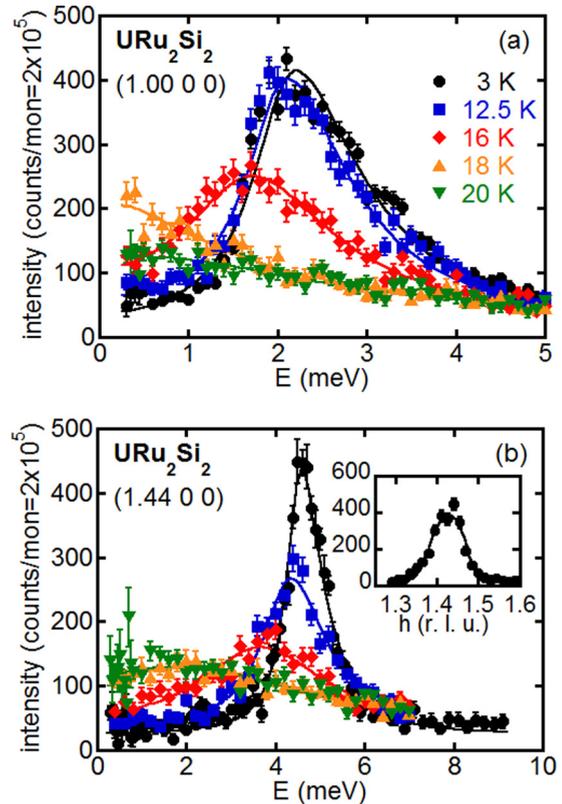

FIG. 1. (Color online) Low-energy excitations. At low temperature T in the hidden-order phase excitations are gapped. Excitations are seen (a) above 2 meV at the commensurate $(1,0,0)$ position and (b) above 4 meV at the incommensurate $(1.44,0,0)$ position. The inset shows an h scan at 4.5 meV at 3 K. Both gaps close at the transition to paramagnetism ($T_0 = 17.5\,K$). (Counting time is approximately 2 min. Solid lines represent damped-harmonic oscillator fits described in the text.)

B. Temperature scans

While the spin fluctuations are not truly critical either at $\vec{Q}_0$ or at $\vec{Q}_1$, we have observed significant differences between the low-energy excitation spectra at $\vec{Q}_0$ and $\vec{Q}_1$ when approaching the onset of hidden order at T_0. For both wave vectors these differences are best visualized in detailed temperature scans at $E = 0.5$ meV (Fig. 2).

At the incommensurate position, $\vec{Q}_1$, the gap opens in a steplike fashion at T_0, with the scattering intensity being essentially constant above T_0. In comparison to related data reported by Wiebe *et al.* [34] for an energy transfer of $E = 0.25$ meV, our scan at $E = 0.5$ meV shows a much sharper decrease of scattering intensity just below T_0. This may be due to larger background contributions at the smaller energy transfer studied by Wiebe *et al.* However, both data sets agree in that there is no enhancement of the low-E excitations when approaching T_0 from above.

In strong contrast, at the commensurate position, $\vec{Q}_0$, the intensity of the low-energy excitations increases below about 24 K when approaching T_0, peaking precisely at T_0. It then decreases in a broad temperature range below T_0, becoming fully suppressed below ~ 11 K.
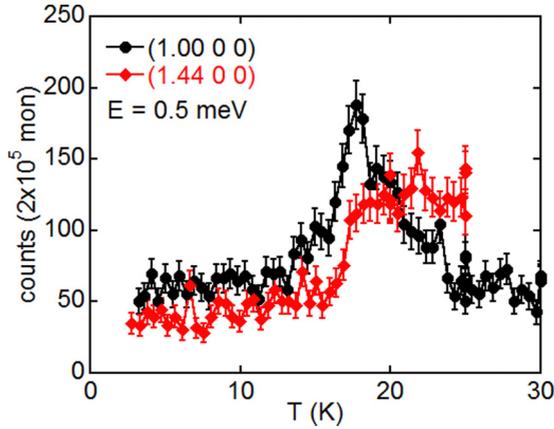
FIG. 2. (Color online) Temperature dependence of the low-energy excitations around the hidden-order to paramagnetic phase transition. At the incommensurate (1.44,0,0) wave vector the gap is filled much more abruptly at T_0, and the $E = 0.5$ meV excitations do not show any additional enhancement. At the commensurate (1,0,0) position the gap is filled across a considerable temperature range around T_0. Low-energy excitations at $E = 0.5$ meV are strongly enhanced and peak precisely at T_0, illustrating the peaking of the damping, which is exclusive to the (1,0,0) position.

C. Analysis of energy scans

The low-energy scattering in Fig. 1 consists of the contribution from the dynamic structure factor $S(\vec{q},E)$ and a background. A main ingredient of $S(\vec{q},E)$ is the imaginary part $\chi''(\vec{q},E)$ of the dynamic susceptibility. In previous studies of the commensurate excitations the imaginary part of the dynamic susceptibility was either modeled as a damped harmonic oscillator [30,38] or, for $T > T_0$, in a quasielastic approximation [30]. Moreover, in a different study, the incommensurate excitations were analyzed below and above T_0 with a Lorentzian model [29]. In comparison, we consistently fit our data at all temperatures at both $\vec{Q}_0$ and $\vec{Q}_1$ using a damped harmonic oscillator function for $\chi''(\vec{q})$:

$$S(\vec{q},E) = \left(\frac{1}{1 - e^{-E/k_BT}}\right)\frac{\chi_0'(\vec{q})E_0^2 D_{\vec{q}}E}{\left(E^2 - E_0^2\right)^2 + D_{\vec{q}}^2 E^2}.$$

Here, $\chi_0'(\vec{q})$ is the real part of the static susceptibility, $D_{\vec{q}}$ denotes damping, and E_0 is the resonance energy of the undamped oscillator. $\left(\frac{1}{1-e^{-E/k_BT}}\right) = n_E + 1$ is the detailed balance factor and contains the Bose-Einstein distribution $n_E = \frac{1}{e^{E/k_BT}-1}$. The detailed balance factor describes the temperature dependence of the probability for neutrons to scatter as a function of energy loss E. In particular, it can be seen that the scattering probability remains significant even if E is much larger than k_BT.

The data in Fig. 1 was fitted using a convolution of $S(\vec{q},E)$ with the resolution ellipsoid, where we have assumed a quadratic dispersion $E_0 = E_0(\vec{Q}_i) + a_{ih}(Q_{ih} - Q_h)^2 + a_{ik}(Q_{ik} - Q_k)^2 + a_{il}(Q_{il} - Q_l)^2$ near both $\vec{Q}_i$, with $i = 0,1$. We have set $\vec{Q}_1 = (1.41,0,0)$ as this is at the boundary of the body-centered tetragonal reciprocal lattice, on which the dispersion minimum seems to be centered [39]. We infer dispersion parameters a_{ih}, a_{ik}, and a_{il} from the results of Broholm et al. [29]. As the dispersion near $\vec{Q}_1$ in the l

direction was not reported in the literature, we have assumed $a_{1l}/a_{1h} = a_{0l}/a_{0h}$. We have assumed χ_0' has a Gaussian $\vec{q}$ dependence in the immediate vicinity of both $\vec{Q}_i$, with $i = 0,1$. We have obtained the strength of the dependence by taking the $\vec{q}$ dependence of the integrated excitation intensity obtained by Broholm et al. [29] at low temperatures as an order of magnitude estimate. For our fits, the resolution ellipsoid was determined in RESCAL [40] with the Cooper-Nathan method with values for the beam divergences derived from the instrument geometry. Fits were obtained by Monte Carlo integrations using MFIT4 [40].

We find that the background, as determined in energy scans at 20 and 3 K at (1.2 0 0), is constant in the E range of our experiment and weakly T dependent. The background is thereby assumed to include the magnetic continuum previously reported in Ref. [30]. The fits shown in Fig. 1 are in excellent agreement with the data, thus supporting the suitability of the model.

The temperature evolution of E_0 and D and the associated resonance energy of the damped oscillator, $E_d = \sqrt{E_0^2 - (D/2)^2}$, are shown in Fig. 3. The condition for critical damping is $E_0 = D/2$, which implies $E_d = 0$. The behaviors of E_0, D, and E_d at $\vec{Q}_0$ and $\vec{Q}_1$ are qualitatively similar. E_0 is fairly constant, with values close to 2 meV at $\vec{Q}_0$ and close to 4 meV at $\vec{Q}_1$. In both cases a small dip is seen near T_0. D strongly increases near T_0, and the damping level changes from moderate below T_0 to critically damped above T_0 in both cases. Near T_0, E_d is suppressed to zero within the error in both cases.

When comparing our results at $\vec{Q}_0$ with the results of previous studies by Mason et al. [38] and Bourdarot et al. [30], the values for E_0 well below T_0 are consistent with each other, and a qualitatively similar increase of D near T_0 is found in each study. However, our observation of only a small dip of E_0 near T_0 is in contrast to the previously reported strong suppression of E_0 near T_0 and to the related equally strong suppression of the resonance energy in a magnetic excitation model [33].

For $\vec{Q}_1$ comparison with other reports is more difficult, as either a three-parameter Lorentzian [5] or a magnetic excitation model [33] was used. Our results for the temperature dependencies of E_0 and D are qualitatively similar to the results found for the resonance energies and damping parameters, respectively, of the previously used models. However, the decrease of E_0 near T_0 in our analysis is comparatively small.

The most striking difference between our study and previous work concerns the T dependence of the resonance energies at $\vec{Q}_0$ compared to $\vec{Q}_1$ across T_0. While Ref. [33] concludes on qualitative differences, we find qualitative similarity between $\vec{Q}_0$ and $\vec{Q}_1$.

We attribute the discussed discrepancies between E_0 and D values for $\vec{Q}_0$ and $\vec{Q}_1$ reported here and in the literature to the following effect: in the regime of stronger damping the harmonic oscillator function only depends on the combination $\Gamma = E_0^2/D$ except at higher E, where the function is close to zero. Therefore, E_0 and D become less well defined as individual fit parameters in the regime of stronger damping. However, Γ itself and the static susceptibility χ_0 are well-defined parameters at any damping level and more appropriate for a comparison of the excitations at $\vec{Q}_0$ and $\vec{Q}_1$. We stress
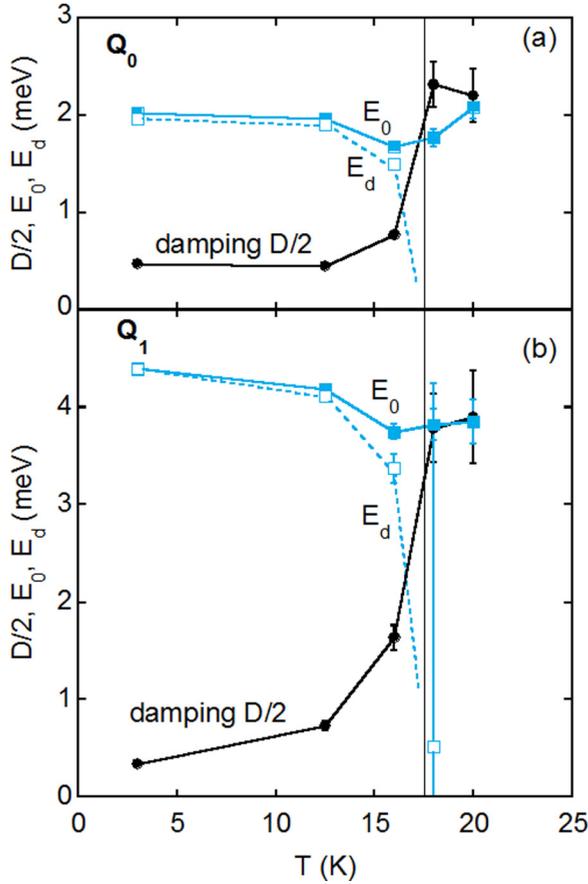
FIG. 3. (Color online) Temperature dependence of the resonance energies of the undamped (E_0) and damped (E_d) oscillators and $D/2$ with damping D. Vertical lines indicate T_0 of the HO-PM transition. The behaviors at (a) the commensurate position $\vec{Q}_0$ and (b) the incommensurate position $\vec{Q}_1$ are qualitatively similar. E_0 is fairly constant and shows a small dip near T_0, while E_d is strongly suppressed near T_0. D shows a significant increase near T_0. The excitations are weakly damped at low temperatures and approximately critically damped ($E_0 \approx D/2$) above T_0. The increased errors at $T > T_0$ reflect that E_0 and D and, in particular, E_d become less well defined near the critically damped regime.

that Γ can only be interpreted as the quasielastic linewidth or relaxation rate of the magnetic excitations in the strongly overdamped limit. Nevertheless, Γ is a meaningful quantity at all damping regimes, as it is true for all levels of damping that an increase in $1/\Gamma$ represents a change to a more highly damped regime (as this depends on the ratio of D and E_0).

Figure 4(a) shows that with increasing T the static susceptibility χ_0 decreases at $\vec{Q}_0$ but increases at $\vec{Q}_1$. The T dependence of $\chi_0(\vec{Q}_0)$ is similar to that reported in Ref. [30]. A divergence as reported by Mason *et al.* [38] is not observed. A comparison of the behavior of $\chi_0(\vec{Q}_1)$ with that in other studies is again more difficult due to the different models used in Refs. [5,33]. Nevertheless, the T dependence of $\chi_0(\vec{Q}_1)$ is found to be qualitatively similar to the amplitude reported in Ref. [5] and the static susceptibility reported in Ref. [33], which are the corresponding parameters of the respective models. To additionally allow for a quantitative comparison
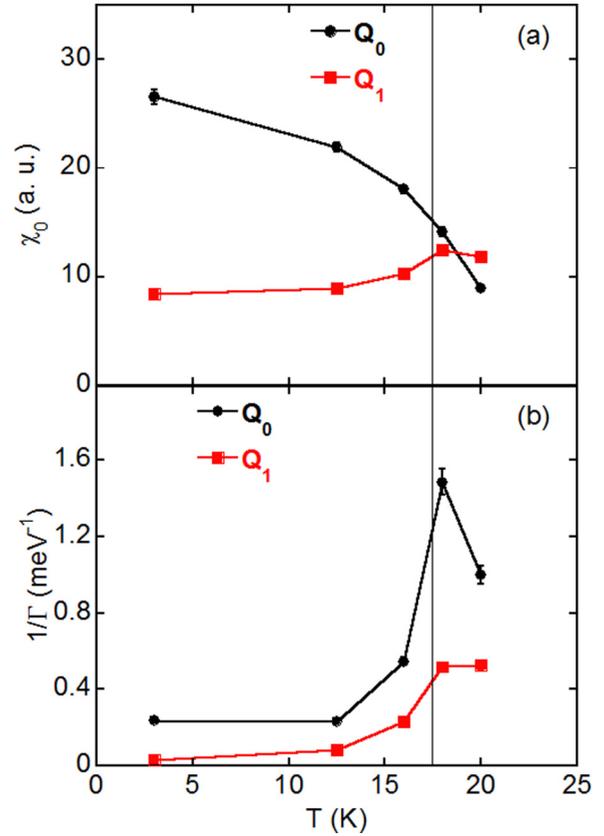

FIG. 4. (Color online) Temperature dependence of (a) the static susceptibility $\chi_0(\vec{q}) = \chi(\vec{q}, \omega = 0)$ and (b) $1/\Gamma$, with $\Gamma = E_0^2/D$. Vertical lines indicate T_0 of the HO-PM transition. (a) $\chi_0(\vec{Q}_0)$ drops while $\chi_0(\vec{Q}_1)$ rises with increasing temperature. $\chi_0(\vec{Q}_0)$ and $\chi_0(\vec{Q}_1)$ have similar magnitudes near T_0. To allow this quantitative comparison of both signals χ_0 values have been normalized by the form factor of UO$_2$ [37]. (b) $1/\Gamma(\vec{Q}_1)$ shows an almost steplike increase near T_0. $1/\Gamma(\vec{Q}_0)$ is larger than $1/\Gamma(\vec{Q}_1)$ in the whole studied temperature range and shows a strong peak at T_0. Γ would correspond to the quasielastic linewidth in the strongly overdamped limit.

of the signals at $\vec{Q}_0$ and $\vec{Q}_1$ in this study, χ_0 values have been normalized by the form factor of UO$_2$ [37]. $\chi_0(\vec{Q}_0)$ has a similar magnitude to $\chi_0(\vec{Q}_1)$ near T_0.

Figure 4(b) shows that the T dependence of $1/\Gamma$, like that of χ_0, is also distinctly different at $\vec{Q}_0$ and $\vec{Q}_1$. In general, at a continuous phase transition, $1/\Gamma$ of the order-parameter response function is expected to diverge. Experimentally, $1/\Gamma(\vec{Q}_0)$, although not diverging, displays a pronounced peak right at T_0. This indicates that the LMAF fluctuations become almost critical at the PM-HO transition, in addition to the expected critical fluctuations of the hitherto unidentified HO parameter. [We note that tiny amounts of quenched disorder may also limit $1/\Gamma(\vec{Q}_0)$ at T_0.]

However, the behavior of $1/\Gamma(\vec{Q}_1)$ is very different. With increasing T, $1/\Gamma(\vec{Q}_1)$ only shows a steplike evolution across T_0. Also, $1/\Gamma(\vec{Q}_1) < 1/\Gamma(\vec{Q}_0)$ in the whole T range studied. A comparison with the raw data in Fig. 2 shows that $1/\Gamma$ captures the main difference between the T dependencies of the low-energy excitation spectra at $\vec{Q}_0$ and $\vec{Q}_1$.

III. DISCUSSION

Our experimental results suggest an intimate relation between the PM-HO phase transition and the commensurate excitations at $\vec{Q}_0$. The latter show enhanced damping towards T_0, much like the critical fluctuations of a second-order magnetic phase transition. In marked contrast, the incommensurate excitations at $\vec{Q}_1$ do not show a peak of $1/\Gamma$. Instead, Γ remains essentially constant when T_0 is approached from high temperatures. The opening of the gap in these incommensurate excitations may in turn be interpreted as a simple *consequence* of the onset of the HO. This view is not incompatible with the proposal [34] that the incommensurate excitations at $\vec{Q}_1$ are mainly responsible for the magnitude of the specific-heat anomaly.

The commensurate fluctuations at $\vec{Q}_0$, although peaked exactly at T_0, do not become critical; that is, the corresponding static susceptibility does not diverge. The latter is only expected if the magnetic order with $\vec{Q}_{\mathrm{AF}} = (0,0,1)$, which is represented by a Bragg peak at $\vec{Q}_0$, becomes static below T_0. This would be the case in the pressure-induced LMAF phase but not in the HO phase. What is then the role of the $\vec{Q}_0$ magnetic fluctuations?

It is instructive to discuss the interplay of hidden order and magnetism using the order-parameter language. If HO and magnetism were to simply represent competing order parameters ψ_{HO} and ψ_{AF}, with ordering wave vectors $\vec{Q}_{\mathrm{HO}}$ and $\vec{Q}_{\mathrm{AF}}$, respectively, an enhancement of the HO would lead to a suppression of magnetism and vice versa. In particular, it would be expected that magnetic fluctuations would be suppressed instead of enhanced when approaching the HO transition. Moreover, one would not expect the HO to couple to the magnetism in a wave-vector-selective manner: to lowest order the allowed coupling in a Landau functional is of the form $|\psi_{\mathrm{HO}}|^2 |\psi_{\mathrm{AF}}|^2$, which does not require any relationship between $\vec{Q}_{\mathrm{HO}}$ and $\vec{Q}_{\mathrm{AF}}$. Therefore, a standard scenario of competing orders with differing symmetries, inferred from the parasitic nature of the small-moment antiferromagnetism and the temperature-pressure phase diagram [9], does not easily account for our data.

This prompts us to invoke a closer relationship between HO and LMAF. Specific proposals along these lines were recently made in Refs. [18,41] for hexadecapolar order and in Ref. [22] for hastatic order. The central idea for such a closer relationship, common to these different microscopic calculations [18,22], is that ψ_{HO} and ψ_{AF} may be treated as components of a *common* supervector order parameter. This implies that the system is in the vicinity of a point with higher symmetry, where HO and magnetism are degenerate. Approaching the ordering transition at T_0 in turn will lead to a concomitant enhancement of *both* HO and magnetic fluctuations, corresponding to nearly isotropic fluctuations in order-parameter space, until, very close to the PM-HO transition, the magnetic fluctuations are cut off, which is consistent with our data. In the simplest case, this scenario suggests $\vec{Q}_{\mathrm{HO}} = \vec{Q}_{\mathrm{AF}} = (0,0,1)$. Therefore, it will be crucial to search for these proposed order parameters [18,22] at wave vector $(0,0,1)$ in the HO phase as well as their fluctuations for $T > T_0$.

IV. CONCLUSIONS

We have shown a strong link between LMAF-related commensurate magnetic fluctuations at $\vec{Q}_0$ and the PM-HO transition in URu$_2$Si$_2$. Temperature scans of the low-energy excitations at the commensurate $\vec{Q}_0$ and the incommensurate $\vec{Q}_1$ positions show qualitatively different behavior across the transition, with the former being strongly enhanced towards the PM-HO transition temperature T_0. An analysis of energy scans in terms of damped harmonic oscillator functions characterized by the resonance energy E_0 and damping D shows that the difference in the temperature scans originates from the temperature dependences of $1/\Gamma = D/E_0^2$ at $\vec{Q}_0$ and $\vec{Q}_1$. Our results put strong constraints on theoretical models for the HO state; they point to a common, nearly isotropic, order-parameter space involving both HO and LMAF order parameters [22,41].

As a consequence we predict for high-pressure neutron scattering experiments of the low-energy excitations near the PM-LMAF transition that the fluctuations at $\vec{Q}_0$ become stronger for increasing pressure at $T_0(p)$, with a clear trend to a truly critical divergence at T_N beyond the bicritical point [9,11–14]. At the same time, the intensity at $\vec{Q}_1$ is predicted to remain noncritical and steplike at all p and T.

Note added in proof. We note two recent Raman spectroscopy reports [42,43] on the observation of a sharp resonance A_{2g} mode at energies very similar to those of the $\vec{Q}_0$ excitations seen in neutron scattering. These works support our supervector-order-parameter interpretation based on Refs. [18,41].

[1] T. T. M. Palstra, A. A. Menovsky, J. van den Berg, A. J. Dirkmaat, P. H. Kes, G. J. Nieuwenhuys, and J. A. Mydosh, Phys. Rev. Lett. **55**, 2727 (1985).

[2] M. B. Maple, J. W. Chen, Y. Dalichaouch, T. Kohara, C. Rossel, M. S. Torikachvili, M. W. McElfresh, and J. D. Thompson, Phys. Rev. Lett. **56**, 185 (1986).

[3] W. Schlabitz, J. Baumann, B. Pollit, U. Rauchschwalbe, H. M. Mayer, U. Ahlheim, and C. D. Bredl, Z. Phys. B **62**, 171 (1986).

[4] J. A. Mydosh and P. M. Oppeneer, Rev. Mod. Phys. **83**, 1301 (2011).

[5] C. Broholm, J. K. Kjems, W. J. L. Buyers, P. Matthews, T. T. M. Palstra, A. A. Menovsky, and J. A. Mydosh, Phys. Rev. Lett. **58**, 1467 (1987).

[6] H. Amitsuka, M. Sato, N. Metoki, M. Yokoyama, K. Kuwahara, T. Sakakibara, H. Morimoto, S. Kawarazaki, Y. Miyako, and J. A. Mydosh, Phys. Rev. Lett. **83**, 5114 (1999).

 [7] K. Matsuda, Y. Kohori, T. Kohara, K. Kuwahara, and T. Matsumoto, J. Phys.: Condens. Matter **15**, 2363 (2003).

 [8] A. Amato, M. J. Graf, A. de Visser, H. Amitsuka, D. Andreica, and A. Schenck, J. Phys.: Condens. Matter **16**, S4403 (2004).

 [9] P. G. Niklowitz, C. Pfleiderer, T. Keller, M. Vojta, Y.-K. Huang, and J. A. Mydosh, Phys. Rev. Lett. **104**, 106406 (2010).

[10] F. Bourdarot, N. Martin, S. Raymond, L.-P. Regnault, D. Aoki, V. Taufour, and J. Flouquet, Phys. Rev. B **84**, 184430 (2011).

[11] G. Motoyama, T. Nishioka, and N. K. Sato, Phys. Rev. Lett. **90**, 166402 (2003).

[12] S. Uemura, G. Motoyama, Y. Oda, T. Nishioka, and N. K. Sato, J. Phys. Soc. Jpn. **74**, 2667 (2005).

[13] E. Hassinger, G. Knebel, K. Izawa, P. Lejay, B. Salce, and J. Flouquet, Phys. Rev. B **77**, 115117 (2008).

[14] G. Motoyama, N. Yokoyama, A. Sumiyama, and Y. Oda, J. Phys. Soc. Jpn. **77**, 123710 (2008).

[15] P. Chandra, P. Coleman, J. A. Mydosh, and V. Tripathi, Nature (London) **417**, 831 (2002).

[16] C. M. Varma and L. Zhu, Phys. Rev. Lett. **96**, 036405 (2006).

[17] A. Kiss and P. Fazekas, Phys. Rev. B **71**, 054415 (2005).

[18] K. Haule and G. Kotliar, Nat. Phys. **5**, 796 (2009).

[19] S. Takagi, S. Ishihara, M. Yokoyama, and H. Amitsuka, J. Phys. Soc. Jpn. **81**, 114710 (2012).

[20] D. D. Khalyavin, S. W. Lovesey, A. N. Dobrynin, E. Ressouche, R. Ballou, and J. Flouquet, J. Phys.: Condens. Matter **26**, 046003 (2014).

[21] S. Elgazzar, J. Rusz, M. Amft, P. M. Oppeneer, and J. A. Mydosh, Nat. Mater. **8**, 337 (2009).

[22] P. Chandra, P. Coleman, and R. Flint, Nature (London) **493**, 621 (2013).

[23] P. S. Riseborough, B. Coqblin, and S. G. Magalhães, Phys. Rev. B **85**, 165116 (2012).

[24] T. Das, Phys. Rev. B **89**, 045135 (2014).

[25] S. Fujimoto, Phys. Rev. Lett. **106**, 196407 (2011).

[26] R. Okazaki, T. Shibauchi, H. J. Shi, Y. Haga, T. D. Matsuda, E. Yamamoto, Y. Onuki, H. Ikeda, and Y. Matsuda, Science **331**, 439 (2011).

[27] S. C. Riggs, M. C. Shapiro, A. V. Maharaj, S. Raghu, E. D. Bauer, R. E. Baumbach, P. Giraldo-Gallo, M. Wartenbe, and I. R. Fisher, Nat. Commun. **6**, 6425 (2015).

[28] S. Tonegawa, S. Kasahara, T. Fukuda, K. Sugimoto, N. Yasuda, Y. Tsuruhara, D. Watanabe, Y. Mizukami, Y. Haga, T. D. Matsuda *et al.*, Nat. Commun. **5**, 4188 (2014).

[29] C. Broholm, H. Lin, P. T. Matthews, T. E. Mason, W. J. L. Buyers, M. F. Collins, A. A. Menovsky, J. A. Mydosh, and J. K. Kjems, Phys. Rev. B **43**, 12809 (1991).

[30] F. Bourdarot, E. Hassinger, S. Raymond, D. Aoki, V. Taufour, L.-P. Regnault, and J. Flouquet, J. Phys. Soc. Jpn. **79**, 064719 (2010).

[31] F. Bourdarot, B. Fåk, V. P. Mineev, M. E. Zhitomirsky, N. Kernavanois, S. Raymond, P. Burlet, F. Lapierre, P. Lejay, and J. Flouquet, arXiv:cond-mat/0312206.

[32] A. Villaume, F. Bourdarot, E. Hassinger, S. Raymond, V. Taufour, D. Aoki, and J. Flouquet, Phys. Rev. B **78**, 012504 (2008).

[33] F. Bourdarot, S. Raymond, and L.-P. Regnault, Philos. Mag. **94**, 3702 (2014).

[34] C. R. Wiebe, J. A. Janik, G. J. MacDougall, G. M. Luke, J. D. Garrett, H. D. Zhou, Y.-J. Jo, L. Balicas, Y. Qiu, J. R. D. Copley *et al.*, Nat. Phys. **3**, 96 (2007).

[35] C. Pfleiderer, J. A. Mydosh, and M. Vojta, Phys. Rev. B **74**, 104412 (2006).

[36] H. Amitsuka, K. Matsuda, I. Kawasaki, K. Tenya, M. Yokoyama, C. Sekine, N. Tateiwa, T. C. Kobayashi, S. Kawarazaki, and H. Yoshizawa, J. Magn. Magn. Mater. **310**, 214 (2007).

[37] B. C. Frazer, G. Shirane, D. E. Cox, and C. E. Olsen, Phys. Rev. **140**, A1448 (1965).

[38] T. E. Mason, W. J. L. Buyers, T. Petersen, A. A. Menovsky, and J. D. Garrett, J Phys.: Condens. Matter **7**, 5089 (1995).

[39] N. P. Butch, M. E. Manley, J. R. Jeffries, M. Janoschek, K. Huang, M. B. Maple, A. H. Said, B. M. Leu, and J. W. Lynn, Phys. Rev. B **91**, 035128 (2015).

[40] Computing for Science Group, RESCAL, Institut Laue Langevin, Grenoble, France.

[41] K. Haule and G. Kotliar, Europhys. Lett. **89**, 57006 (2010).

[42] H.-H. Kung, R. E. Baumbach, E. D. Bauer, V. K. Thorsmølle, V.-L. Zhang, K. Haule, J. A. Mydosh, and B. Blumberg, Science **347**, 1339 (2015).

[43] J. Buhot, M.-A. Méasson, Y. Gallais, M. Cazayous, A. Sacuto, G. Lapertot, and D. Aoki, Phys. Rev. Lett. **113**, 266405 (2014).